

Mechanical Relaxations and Moduli of Isotropic and Oriented Linear Low-Density Polyethylene

C. L. CHOY and W. P. LEUNG, *Department of Physics, The Chinese University of Hong Kong, Hong Kong* and H. C. NG,* *Department of Chemistry, The Chinese University of Hong Kong, Hong Kong*

Synopsis

The mechanical relaxations of isotropic and oriented linear low-density polyethylene have been studied between -180 and 90°C by the use of a torsion pendulum (1 Hz), a dynamic tensile apparatus (5–90 Hz), and a longitudinal wave attenuation technique (10 MHz). The five independent elastic moduli of the oriented samples have also been measured from -60° to 50°C by an ultrasonic method. Wide-angle X-ray diffraction and birefringence measurements reveal that the chains in the crystalline phase are fully aligned at draw ratio $\lambda = 4$, but the degree of amorphous orientation increases steadily, indicating that the number of well-aligned tie molecules continues to increase up to the highest attainable draw ratio ($\lambda = 6.1$). The slight depression of the γ and β relaxation peaks upon drawing results from a lowering of molecular mobility in the amorphous and interfacial regions due to the constraining effect of taut tie molecules. At low temperature, the sharp rise in the axial Young's modulus E_0 and slight drop in the transverse modulus E_{90} with increasing λ largely reflects the overall chain orientation. Just above the β relaxation, the stiffening effect of taut tie molecules leads to increases in all moduli including the shear moduli. The two-phase Reuss (uniform stress) model provides an adequate description of the elastic anisotropy only at $\lambda < 3$, mainly because the internal stress distribution in a highly oriented sample is not uniform but corresponds to a situation intermediate between uniform stress and uniform strain field.

INTRODUCTION

Linear low-density polyethylene (LLDPE) is a recently introduced commercial polymer which has shown great promise.^{1–7} This material has improved tensile strength and elongation characteristics, higher stiffness at a given density, and better heat and stress crack resistance compared to conventional highly branched low-density polyethylene produced by high-pressure polymerization processes. Since LLDPE contains little or no long-chain branches, it is more readily stretched, and is therefore commonly used to produce oriented structures. Although there are a number of articles in trade journals^{1–7} describing the engineering properties of LLDPE, there are as yet very few basic studies of the solid state properties of isotropic and oriented LLDPE. The relaxations of isotropic LLDPE have been investigated by dynamic birefringence⁸ and mechanical^{8,9} techniques and the effect of drawing¹⁰ or extrusion¹¹ on the tensile modulus has been reported.

In the present work, the development of chain orientation in LLDPE upon drawing is followed by wide-angle X-ray diffraction and birefringence measurements. The mechanical relaxations in isotropic and drawn LLDPE are

*Present address: Research Centre, Du Pont Canada Inc., Kingston, Ontario, Canada.

also studied between -180 and 90°C by using a torsional pendulum at 1 Hz, a dynamic tensile apparatus from 5 to 90 Hz, and a longitudinal wave attenuation method at 10 MHz. Moreover, the five independent elastic moduli of drawn LLDPE have been measured from -60 to 50°C using an ultrasonic wave technique. Attempts are made to correlate the changes in mechanical properties with the increase in the degree of chain orientation in the material.

EXPERIMENTAL

Sample Preparation

The material used is an ethylene-1-butene copolymer (SCLAIR 91 A), containing an estimated 4 ethyl sidegroups per 100 main-chain carbon atoms and has a melting point of about 120°C . The number and weight average molecular weights are 2.37×10^4 and 12.3×10^4 , respectively. This material is produced commercially by DuPont Canada Inc. using a low-pressure solution process with a catalyst system similar to that patented by Elston,¹² which gives homogeneous copolymers of ethylene and 1-alkenes. Ideally, all molecules in such homogeneous copolymers should possess a random distribution of comonomer units and they should have the same comonomer/ethylene ratio.¹² For an analogous series of copolymers prepared using the same Elston catalyst, it has been inferred from the simplicity of the ^{13}C -NMR spectra and from the melting behavior that the branches are randomly distributed.¹³

Pellets of this linear low-density polyethylene were compression-molded at 160°C and then quenched in water at room temperature. Oriented samples were prepared by drawing the isotropic sheets at 65°C on a Instron tensile machine at a rate of 1 cm/min. To ensure that there is no structural change during the course of the experiment, samples for ultrasonic measurements were annealed for 2 h at 50°C , the upper temperature limit of our measurements.

Sample Characterization

The samples were examined in a Leitz optical microscope with crossed polarizers. The density ρ of the samples was determined by the flotation method using mixtures of toluene and carbon tetrachloride, and the volume-fraction crystallinity X_ρ was calculated from the expression:

$$X_\rho = \frac{\rho - \rho_a}{\rho_c - \rho_a}$$

where ρ_c and ρ_a are the density of the crystalline and amorphous phase. The enthalpy of fusion H was measured on a Perkin-Elmer DSC-2 differential scanning calorimeter at $10^\circ\text{C}/\text{min}$ and the volume-fraction crystallinity was calculated from the equation:

$$X_{\text{DSC}} = \frac{\rho H}{\rho_c H_c}$$

where H_c , the enthalpy of fusion of polyethylene crystals, is taken to be 69 cal/g.¹⁴

Wide-Angle X-Ray Diffraction and Birefringence

The azimuthal intensity distribution of the X-ray reflection from the (002) planes was recorded with a Syntex R3 diffractometer and the crystalline orientation function was calculated using a standard method.¹⁵ Birefringence measurements were carried out at room temperature with a Leitz polarizing microscope equipped with a tilting compensator.

Mechanical Measurements

Dynamic torsional measurements about the draw axis of the oriented samples were carried out on an inverted torsional pendulum at 1 Hz. Dynamic tensile measurements at 0°, 45°, and 90° to the draw axis were made on a viscoelastic spectrometer (Iwamoto Seisakusho Ltd.) from 5 to 90 Hz. The temperature range covered by these low-frequency measurements was from -180 to 90°C.

Ultrasonic measurements at 10 MHz were made between -60 and 50°C by using an immersion technique, the details of which had been described previously.^{16,17} All five independent elastic moduli were determined and other parameters including Young's modulus and Poisson's ratios were calculated. Because of the strong attenuation of shear waves it was not possible to carry out modulus measurements above 50°C. The loss tangent was obtained from the attenuation of longitudinal wave. For the oriented sample, the direction of propagation was normal to the draw axis.

RESULTS AND DISCUSSION

Sample Morphology and Characterization

Under the polarizing microscope, the undrawn sample exhibits a spherulitic morphology, with the diameter of the spherulites in the range of 3–20 μm . According to Peterlin,¹⁸ the spherulites are deformed and then broken up as a semicrystalline polymer is drawn. Crystalline blocks are torn off from the lamellae and are connected by taut tie molecules originating from partial unfolding of chains. The alternating amorphous and crystalline regions, together with the taut tie molecules, form long, thin (about 100 Å width) microfibrils which are aligned in the draw direction. We have observed that the spherulites in LLDPE completely disappear at a draw ratio λ above 2.6, which is consistent with Peterlin's result that microfibril formation begins at about $\lambda = 2$.

As shown in Table I, the density ρ of LLDPE increases with increasing draw ratio λ . Taking the density of the crystalline and amorphous phase to be

TABLE I
Density and Crystallinity of Linear Low-Density Polyethylene Samples

Draw Ratio		1	1.4	2.6	3.6	4.4	5.3	6.1
Density	(g cm^{-3})	0.919	0.919	0.920	0.921	0.924	0.923	0.925
Crystallinity	X_p	0.441	0.441	0.448	0.455	0.476	0.469	0.483
	X_{DSC}	0.381	0.392	0.377	0.400	0.429	0.413	0.430

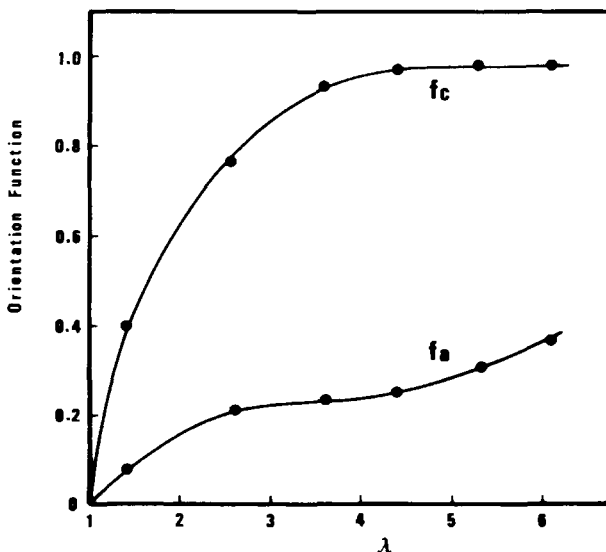


Fig. 1. Draw ratio dependence of the crystalline (f_c) and amorphous (f_a) orientation functions of oriented LLDPE. f_a is calculated from the birefringence by taking $\Delta_c^0 = 0.0585$ and $\Delta_a^0 = 0.0735$.

1.000 and 0.855, respectively,¹⁹ and assuming that they remain unchanged upon orientation the volume-fraction crystallinity X_p has been calculated and found to increase by about 10% as λ rises from 1 to 6.1. It should be cautioned that the assumption of constant density for the amorphous phase may not be a good one, especially at high draw ratio. However, the crystallinity X_{DSC} deduced from the enthalpy of fusion also supports the conclusion that there is a slight increase in the crystalline content upon orientation.

Wide-Angle X-Ray Diffraction and Birefringence

The crystalline orientation function f_c determined from wide-angle X-ray diffraction is shown as a function of draw ratio λ in Figure 1. The crystalline orientation function rises sharply in the range $\lambda = 1-3$ and becomes saturated at higher λ , indicating that the chains in the crystalline regions are fully aligned above $\lambda = 4$. At low draw ratio, the birefringence Δ exhibits a behavior similar to that of f_c . At $\lambda \geq 4$, however, Δ shows a slower but continued increase up to the highest attainable draw ratio (Fig. 2).

Neglecting form birefringence, Δ can be expressed as

$$\Delta = Xf_c\Delta_c^0 + (1 - X)f_a\Delta_a^0$$

where X is the volume fraction crystallinity, f_c and f_a are the crystalline and amorphous orientation function, and Δ_c^0 and Δ_a^0 are the intrinsic birefringence of the crystalline and amorphous phase. Taking $\Delta_c^0 = 0.0585$ ²⁰ and using crystallinity values deduced from the density data, we have calculated the crystalline contribution $Xf_c\Delta_c^0$. This term, and the amorphous contribution $(1 - X)f_a\Delta_a^0$, obtained by subtracting $Xf_c\Delta_c^0$ from the observed Δ , are plotted

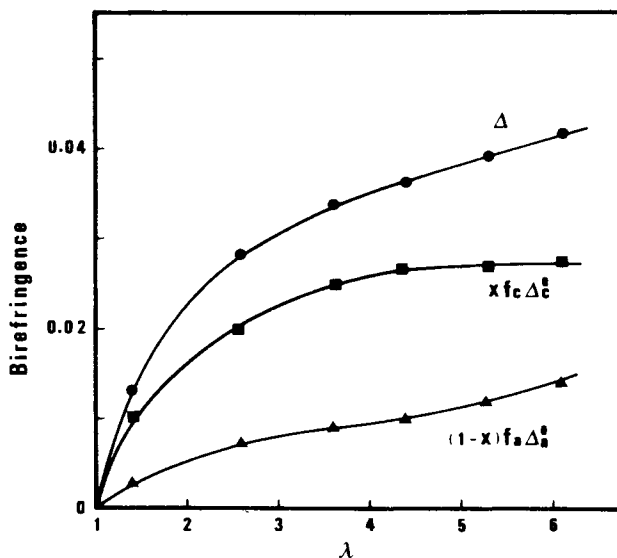


Fig. 2. Draw ratio dependence of the birefringence of oriented LLDPE.

as functions of draw ratio in Figure 2. It is seen that the crystalline phase provides the major contribution to the total birefringence.

The amorphous orientation function f_a is an important quantity since it is a quantitative measure of the alignment of tie molecules as well as other types of chain segments (including floating chains, cilia, and chain folds) in the amorphous regions. The mechanical behavior at low draw ratio is influenced by the orientation of the various kinds of chain segments. At high draw ratio, however, the elastic modulus, particularly the axial Young's modulus, is largely determined by the taut tie molecules.¹⁸ To calculate f_a from the X-ray and birefringence data the intrinsic birefringence of the amorphous phase Δ_a^0 must be known. Although various estimates of Δ_a^0 for polyethylene have been reported in the literature,²¹⁻²³ the values differ considerably. From strain-optical studies at low draw ratio ($\lambda = 1.02-1.05$) Fukui et al.²¹ obtained $\Delta_a^0 = 0.26$ for LDPE. For LLDPE sample at $\lambda = 6.1$ this Δ_a^0 value leads to $f_a = 0.1$, which is much lower than the typical values of 0.4-0.5 obtained for various polymers (polypropylene,^{17,24} polyoxymethylene,²⁵ and nylon 6²⁶) at a similar draw ratio. Therefore, we have to agree with Pietralla et al.²² that this Δ_a^0 value is not appropriate for highly oriented polyethylene. Nakayama and Kanetsuna²³ suggested a value of 0.0485, calculated from $\Delta_a^0 = \Delta_c^0 \rho_a / \rho_c$ on the assumption that the internal-field effects may be neglected. This value is not correct since Hong et al.²⁷ and Pietralla et al.²² have shown that for polyethylene Δ_a^0 will be greater than Δ_c^0 because of internal-field effects.

More reliable estimates have been provided by Pietralla et al.,²² who considered various model nematic-like structures for a well-oriented amorphous polymer. Following a proposal of Pechhold and Grossman,²⁸ they assumed that the amorphous phase in polyethylene has a mixture of 1/3 planar chains and 2/3 helical chains and obtained $\Delta_a^0 = 0.0735$ and 0.0903, respectively, by using the "homogeneous" and "heterogeneous" models, which correspond to

the cases of highly perfect and highly defective structures. We have used a Δ_a^0 value of 0.0735 in our calculation since the resulting f_a 's shown in Figure 1, are more comparable to the values obtained for other semicrystalline polymers.^{17,24-26} It is apparent from Figure 1 that f_a continues to increase at $\lambda > 4$, where the crystalline orientation becomes saturated. This reflects a steady increase in the degree of orientation of the amorphous chain segments and in the number of well-aligned tie molecules up to the highest attainable draw ratio.

Mechanical Relaxations

Figure 3 shows the loss modulus and loss tangent of isotropic LLDPE as functions of temperature at three frequencies, 1 Hz, 90 Hz, and 10 MHz. At low frequency three mechanical relaxations α , β , and γ are observed in the $\tan \delta$ plot. The β process, however, is rather weak and appears only as slight bump near the low-temperature tail of the α process. On the other hand, the β relaxation is very conspicuous in the loss modulus plot. The α relaxation is not seen in the high frequency measurements since it is located above 100°C,²⁹ outside the range of our experiment.

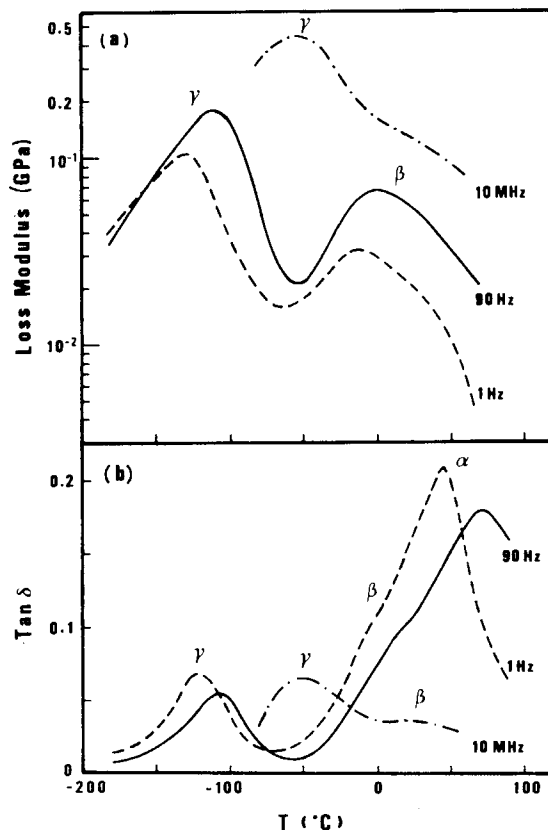


Fig. 3. Temperature dependence of the (a) loss modulus and (b) loss tangent of isotropic LLDPE at frequencies of 1 Hz, 90 Hz, and 10 MHz.

It is generally agreed^{29,30} that the γ relaxation is associated with the amorphous phase. Although the mechanically active α process requires the presence of the crystalline phase, Boyd²⁹ has recently shown that the relaxation strength can also be attributed to the deformation of amorphous regions. The assignment of the β relaxation is still controversial. From the analysis of the mechanical loss and moduli as functions of crystallinity in terms of models for composite materials, Boyd has inferred that the β process occurs in the amorphous phase. On the other hand, Mandelkern and co-workers³¹ studied a variety of polyethylene samples of different structures by combining Raman spectroscopy with dynamic mechanical measurements and concluded that it is the chain segments in the interfacial regions which are responsible for the β relaxation. Our limited data on one isotropic sample does not provide any new information which would help to resolve this issue.

The effect of orientation on the relaxation behavior is shown in the torsional measurements in Figure 4. The β and γ peaks are slightly depressed upon orientation, but the most prominent feature is the large increase in the magnitude of the α peak and the downward shift of its temperature location. The reduction in height of the β and γ relaxations implies that the motion of

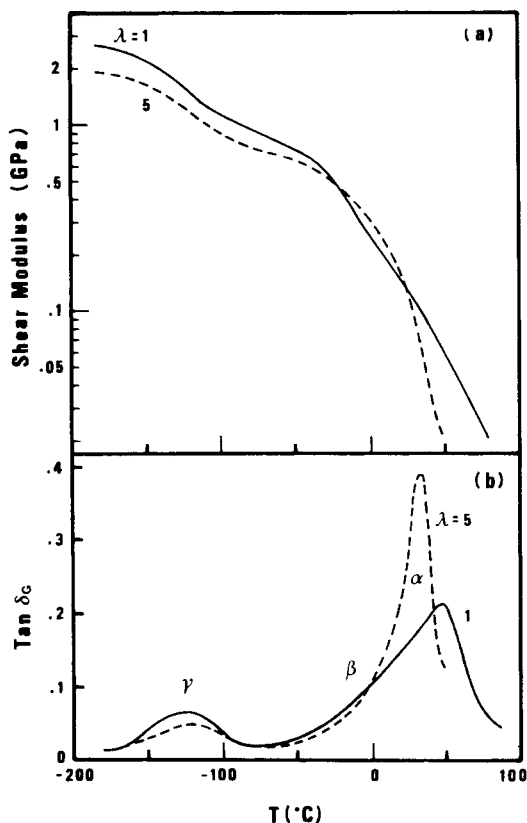


Fig. 4. Effect of orientation on the (a) shear modulus and (b) loss tangent of LLDPE obtained from torsional measurements at 1 Hz. For the oriented sample ($\lambda = 5$) the axis of torsion is parallel to the draw axis.

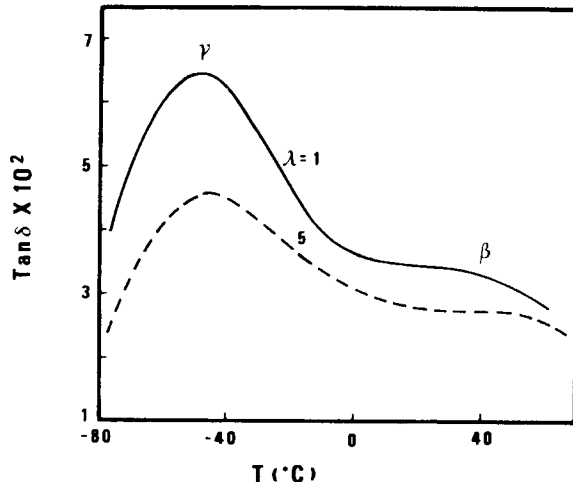


Fig. 5. Effect of orientation on the ultrasonic loss factor of LLDPE at 10 MHz. The data were obtained from measurements of longitudinal wave attenuation. For the oriented sample ($\lambda = 5$) the direction of propagation is normal to the draw axis.

chain segments in the amorphous and interfacial regions is constrained because of the presence of taut tie molecules. This is consistent with the decrease in the sorption and diffusion coefficient recently observed.³² The lowering of these two peaks is also clearly displayed in the ultrasonic measurements (Fig. 5). The strong α process was previously observed³³ in drawn branched low-density polyethylene and was ascribed to shear deformation in planes containing the chain axis (*c*-shear process).

At low temperature, the oriented sample has a lower shear modulus [Fig. 4(a)]. However, as a result of the stiffening effect of taut tie molecules, the axial shear modulus of oriented LLDPE drops more gently with increasing temperature so that, just above the β relaxation, it is higher than the modulus for the isotropic material. With further increase in temperature the strong *c*-shear process at the α relaxation leads to a very low shear modulus for the oriented sample.

The anisotropy of the Young's modulus and mechanical relaxations is shown in Figure 6. At low temperature, the Young's modulus of the oriented sample along the draw axis E_0 is much higher than that in the transverse direction E_{90} , and this is a consequence of the chain alignment in both the crystalline and amorphous regions. However, E_0 drops more drastically with increasing temperature so that $E_0 \approx E_{90}$ above the β relaxation. This behavior has been previously observed and explained by Takayanagi et al.³⁴ For an oriented sample, the crystalline and amorphous regions are arranged in series along the draw axis, and so the application of stress along this direction would give a large fall at the major amorphous relaxation. In the transverse direction where the crystalline and amorphous regions are parallel, the drop in modulus is smaller since the crystalline phase still supports the applied stress. Since the tie molecules are not relaxed, E_0 would not fall below E_{90} .

Figure 6 also reveals that, at low temperature, E_{45} is slightly lower than E_{90} . Moreover, E_{45} drops sharply at the α relaxation so that, above 50°C, E_{45}

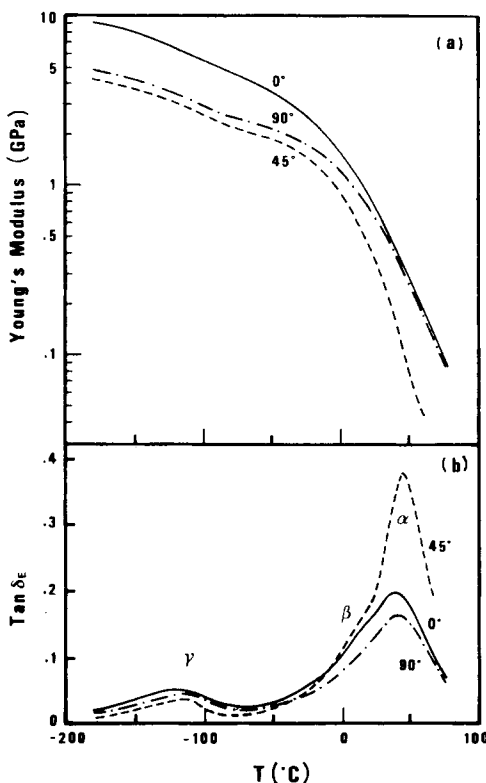


Fig. 6. Temperature dependence of the (a) Young's modulus and (b) loss tangent of oriented LLDPE ($\lambda = 3.6$) at 0° , 45° , and 90° to the draw axis. The data were obtained from tensile measurements at 10 Hz.

is more than 3 times smaller than E_{90} . The large drop in E_{45} and the accompanying high $\tan \delta$ peak further confirm the assignment of the c -shear mechanism to the α relaxation.

Ultrasonic Moduli

The ultrasonic method has advantages over the low-frequency techniques in that it can be applied to small samples (typically $12 \times 10 \times 0.7 \text{ mm}^3$ in the present work) and it can provide all five independent elastic moduli necessary for the complete characterization of an uniaxially oriented material. Our measurements were confined to the range -60 – 50°C since the strong attenuation of shear waves in LLDPE prevented us from working at higher temperatures. This temperature range corresponds to the region from just below the γ relaxation to slightly above the β relaxation (see Fig. 3). Figure 7 shows the various elastic moduli as functions of temperature for an oriented sample at draw ratio $\lambda = 6.1$. The axial extensional modulus (C_{33}), the axial (C_{44}), and transverse (C_{66}) shear modulus have rather strong temperature dependence but the cross-plane moduli C_{13} and C_{12} decreases only by 30% over the entire temperature range. The axial extensional modulus C_{33} is higher than the transverse modulus C_{11} , reflecting the preferential alignment of

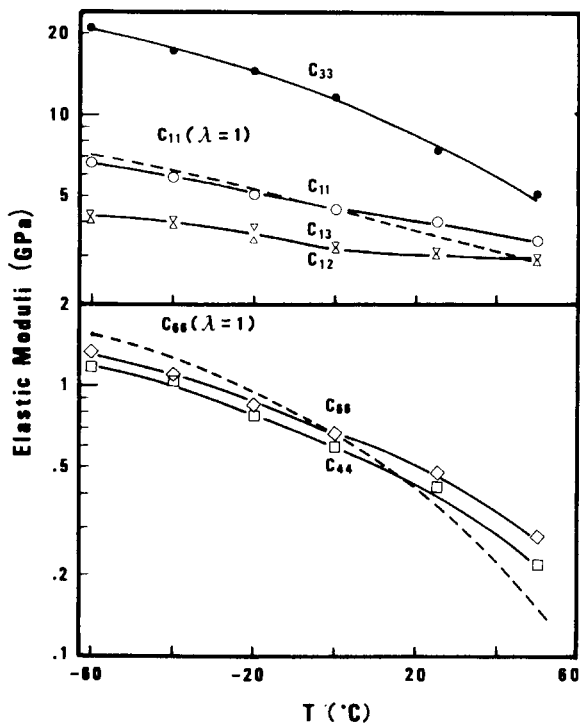


Fig. 7. Temperature dependence of the elastic moduli of oriented LLDPE ($\lambda = 6.1$). The elastic moduli of isotropic LLDPE, C_{11} and C_{66} , are also shown as dashed lines.

chains along the draw axis. The fact that the axial shear modulus C_{44} is lower than the transverse shear modulus C_{66} indicates that the c -shear process may have an effect even at temperatures much lower than the α relaxation.

Figure 8 reveals that the axial Young's modulus E_0 increases sharply with increasing draw ratio. We have seen from Figure 1 that the crystalline chains are completely aligned at $\lambda = 4$, so that the substantial increase in E_0 above this draw ratio must be associated with the increase in the number of taut tie molecules. The transverse modulus E_{90} is much smaller than E_0 and has a weaker temperature dependence, especially at the β relaxation ($\approx 40^\circ\text{C}$). As a result, the anisotropy factor E_0/E_{90} for the highly oriented sample ($\lambda = 6.1$) decreases from about 4 at -60°C to 2.5 at 50°C . Like the low-frequency data in Figure 6, this behavior can also be explained on the basis of the Takayanagi model.³⁴

Since the changes in moduli upon orientation may reflect different mechanisms at different temperatures, we have plotted various moduli as functions of draw ratio at two temperatures, -60 and 50°C (Figs. 9 and 10). At low temperature, the sharp increase in the axial moduli, C_{33} and E_0 , and the slight decrease in the transverse moduli, C_{11} , C_{66} , and E_{90} , merely reflect the continued increase in the overall chain orientation. The c -shear process also seems to have a small effect and gives rise to the slight decrease in C_{44} and E_{45} . At 50°C (just above the β relaxation) the constraining effect of taut tie molecules comes into play, thereby leading to increases in all elastic moduli.

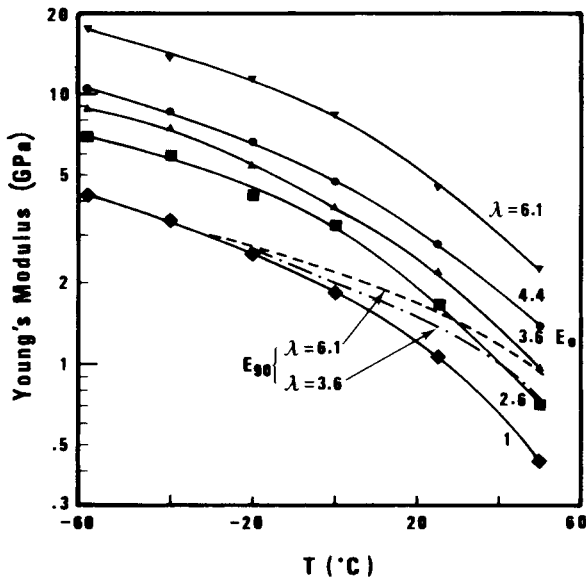


Fig. 8. Temperature dependence of the axial and transverse Young's modulus of oriented LLDPE.

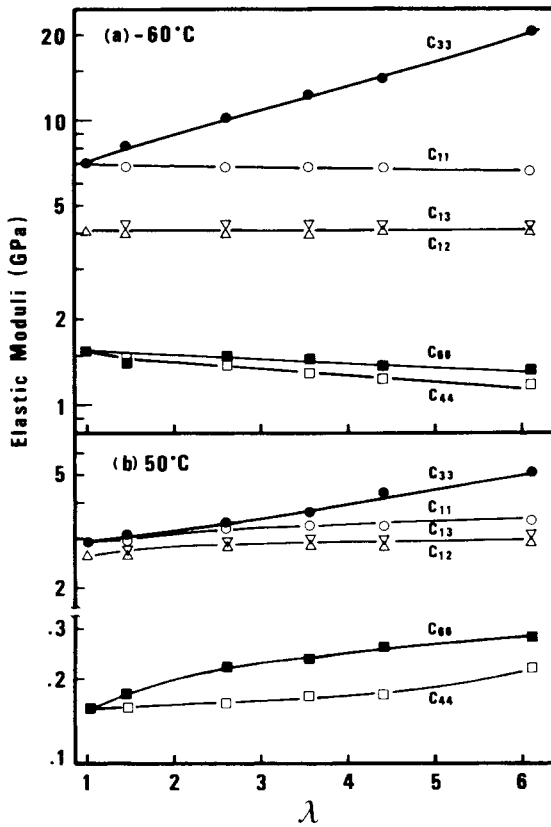


Fig. 9. Draw ratio dependence of the elastic moduli of oriented LLDPE at (a) -60°C and (b) 50°C .

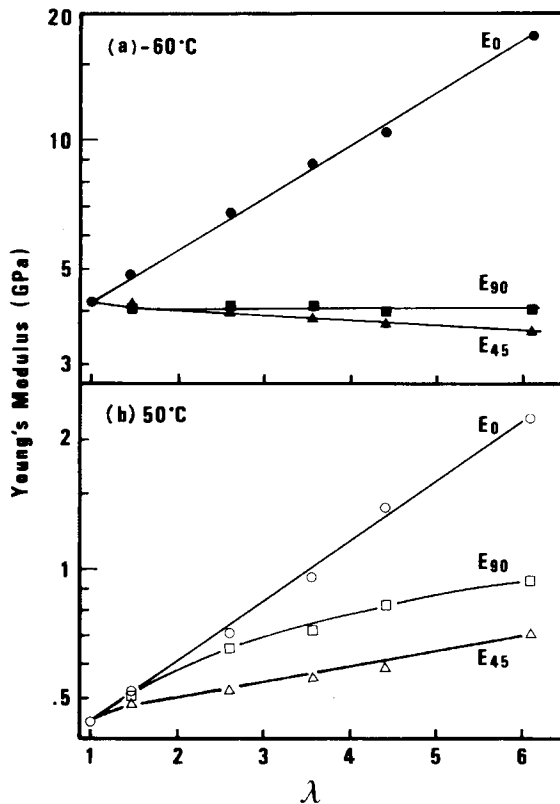


Fig. 10. Draw ratio dependence of the Young's modulus of oriented LLDPE at 0°, 45°, and 90° to the draw direction: (a) -60 and (b) 50°C.

The influence of the three mechanisms is also apparent in the plot of the Young's modulus as a function of the angle with respect to the draw direction (Fig. 11). The anisotropy pattern $E_0 > E_{90}$ reflects the chain orientation but the small minimum near an angle of 50° is caused by the c -shear process. At 50°C, the Young's modulus of the oriented sample at all angles is higher than that for the isotropic material, indicating that the amorphous regions are stiffened as a result of drawing.

Other engineering parameters such as Poisson's ratios are commonly used to characterize an anisotropic material, and it is interesting to see how they are affected by drawing. Figure 12 shows that ν_{21} increases and ν_{31} decreases significantly with increasing draw ratio while ν_{13} exhibits little change. For a highly oriented sample ($\lambda = 6.1$) ν_{21} is much larger than ν_{31} , implying that under transverse tensile stress the sample will deform predominantly in the transverse plane with little contraction along the draw direction. Similar behavior has been observed in our previous work on high-density polyethylene,³⁵ polyoxymethylene,²⁵ and polypropylene.¹⁷

Comparison with Two-Phase Aggregate Model

For an amorphous or slightly crystalline polymer, the mechanical anisotropy is largely determined by the chain orientation. Ward³⁶ proposed a

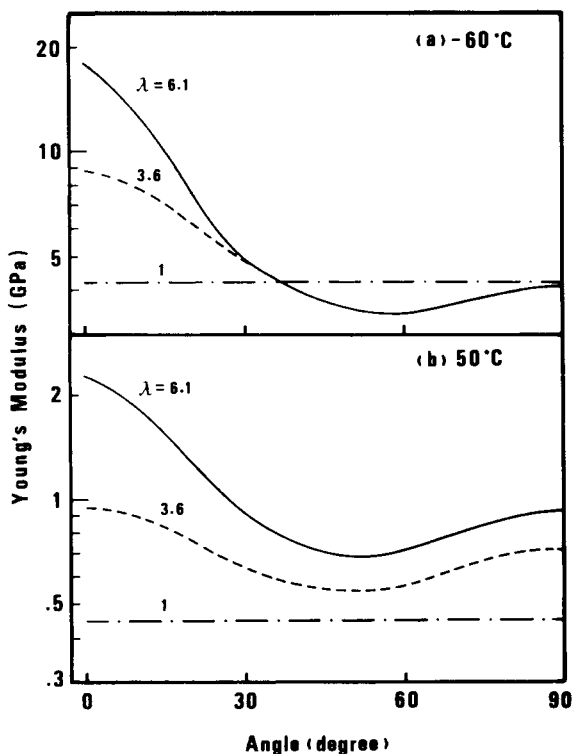


Fig. 11. Variation of the Young's modulus of oriented LLDPE as a function of the angle relative to the draw direction. (a) -60 and (b) 50°C .

model which regarded a polymer as an aggregate of anisotropic units, whose properties remain constant, but are gradually aligned as the polymer is drawn. The calculation of elastic constants can be made in two ways, either by assuming uniform stress (Reuss average) or uniform strain (Voigt average). The Reuss and Voigt procedures involve averaging the compliance constants and stiffness constants, respectively, giving the lower and upper bounds for the elastic constants of the oriented polymer.

Recently, there have been several attempts³⁷⁻⁴² to combine the essential features of the aggregate model and models for composite materials. Since the underlying ideas of these approaches are similar, we will only discuss the model of McCullough et al.⁴⁰ A semicrystalline polymer is regarded as consisting of crystalline and amorphous aggregates of elastic anisotropic units. If the elastic properties of the individual crystalline and amorphous units are known, the elastic constants of each aggregate (crystalline or amorphous) can be calculated through an averaging procedure which takes into account the orientation of the units and the internal stress-strain distribution. Finally, the elastic tensor of the polymer can be calculated by volume averaging of the properties of the crystalline and amorphous aggregates according to micro-mechanical models consistent with the stress-strain field between the aggregate phases.

There are two major difficulties which hamper the comparison with experimental results. First, because the elastic tensor for the intrinsic units in the

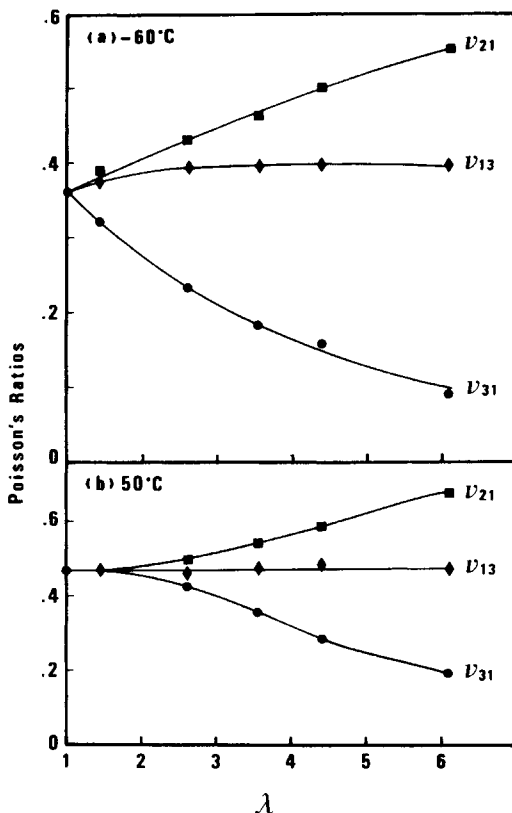


Fig. 12. Draw ratio dependence of the Poisson's ratios of oriented LLDPE at (a) -60 and (b) 50°C .

amorphous phase is unknown, the amorphous phase is often assumed to be isotropic and its elastic properties are obtained from extrapolations of the data for isotropic samples at various crystallinity.^{40,41} While this assumption is reasonable at very low draw ratio or for annealed samples, it is certainly not valid for highly oriented polymers. An even more serious difficulty is the lack of knowledge of the internal stress-strain distribution in semicrystalline polymers. As a result, McCullough et al.⁴⁰ were forced to adopt a bounding approach. Unfortunately, the Reuss and Voigt bounds are generally very far apart. To remedy this situation, they followed the fibrous composite theory approach of Tsai et al.⁴³ and introduced a contiguity factor to express movement between the lower and upper bounds caused by changes in size, shape, packing geometry, and properties of the individual phases. However, as far as we know, there are no existing models or structural techniques which would give the contiguity factor of an oriented semicrystalline sample.

Tighter bounds can be obtained if a specific morphology is assumed. This has been amply demonstrated by Boyd,⁴² who considered a local morphology of stacked lamellae and assumed that the amorphous phase is isotropic. This model is not applicable to highly oriented polymers since it is well known that the morphology is fibrillar and the chains in the amorphous phase have a significant degree of orientation.

We have seen that there are serious difficulties in the application of the general two-phase aggregate model to semicrystalline polymers over a wide range of chain orientation. Fortunately, as pointed out by McCullough, Seferis, and Samuels,^{40,41} semicrystalline polymers processed by traditional means tend to follow the Reuss model. Since the tensile behavior (especially the axial tensile modulus E_0) is sensitively dependent on orientation, we will analyze these data using the Reuss averaging procedure which gives the tensile compliances^{40,41}:

$$\langle S_{ij} \rangle = X \langle S_{ij} \rangle_c + (1 - X) \langle S_{ij} \rangle_a \quad (1a)$$

with

$$\langle S_{33} \rangle_p = A_p + B_p f_p + C_p g_p \quad (1b)$$

$$\langle S_{11} \rangle_p = A_p - \frac{1}{2} (B_p + \frac{5}{4} C_p) f_p + \frac{3}{8} C_p g_p \quad (1c)$$

The subscript p denotes the crystalline (c) or amorphous (a) phase, X represents volume fraction of crystalline phase, and f_p and g_p are, respectively, the second and fourth moment of the distribution of chain orientation:

$$f_p = \frac{1}{2} (3 \langle \cos^2 \theta \rangle_p - 1) \quad (2a)$$

$$g_p = \frac{1}{4} (5 \langle \cos^4 \theta \rangle_p - 1) \quad (2b)$$

with θ being the angle between the chain and draw axis.

The six parameters A_p , B_p , and C_p are related to the compliances of the crystalline and amorphous units, and it is not possible to find all their values since the compliances of the amorphous units are not known. By making the reasonable assumptions that (i) the axial tensile compliance of each phase (crystalline or amorphous) is equal to zero and (ii) the axial shear compliance and the transverse tensile compliance of each phase are approximately equal, eq. (1) reduces to a two-parameter form^{40,41}:

$$E_0^{-1} = X A_c (1 - f_c) + (1 - X) A_a (1 - f_a) \quad (3a)$$

$$E_{90}^{-1} = X A_c (1 + f_c/2) + (1 - X) A_a (1 + f_a/2) \quad (3b)$$

For an isotropic polymer, $f_c = f_a = 0$; therefore,

$$E_{\text{iso}}^{-1} = X A_c + (1 - X) A_a \quad (3c)$$

By considering the limiting cases, $X = 1$, $f_c = 1$ and $X = 0$, $f_a = 1$, eq. (3b) gives

$$A_c = 2/3 E_{\perp}^c \quad (4a)$$

$$A_a = 2/3 E_{\perp}^a \quad (4b)$$

where E_{\perp}^c and E_{\perp}^a are the transverse tensile modulus of the crystalline and

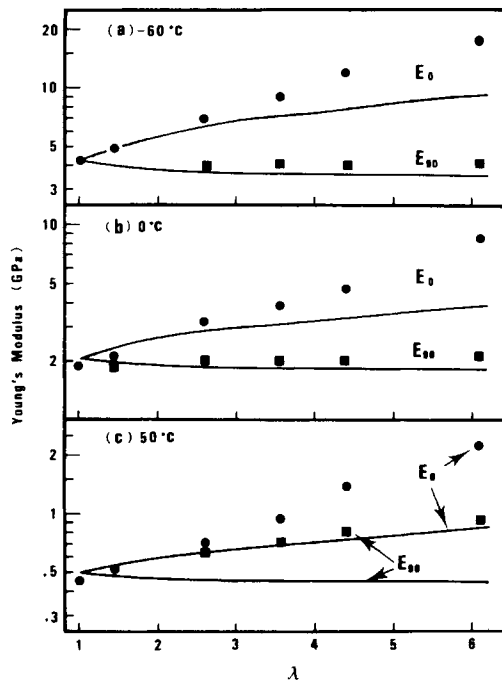


Fig. 13. Draw ratio dependence of the axial and transverse Young's modulus of oriented LLDPE at (a) -60°C , (b) 0°C , and (c) 50°C . The symbols are data points and the solid curves denote theoretical values calculated from the two-phase Reuss model.

amorphous phase, respectively. It should be emphasized that eq. (3) is only a specialized form of the Reuss expression of McCullough et al. obtained by making several reasonable assumptions. This is done to reduce the number of parameters from six to two, which can then be deduced from the data for isotropic samples.

We have obtained ultrasonic data for a series of isotropic Sclair polyethylene samples³² with crystallinity ranging from 0.44 to 0.8 and have fitted the tensile compliance against crystallinity to a straight line to give A_c and A_a . Above the γ relaxation, the compliance of the isotropic sample is increasingly dominated by the $(1 - X)A_a$ term in eq. (3c) and so the fit is not sensitively dependent on A_c . To avoid obtaining unrealistic values for A_c , we have deduced this parameter by fitting the data at -60°C and assumed that it is independent of temperature. The value of E_\perp^c thus obtained is 5.8 GPa, which is in reasonable agreement with the experimental results of 4–6 GPa and theoretical estimates of 6–9 GPa.⁴⁴ The values of E_\perp^a are 2.0, 0.86, and 0.19 GPa at -60 , 0 and 50°C , respectively.

Using these E_\perp^c and E_\perp^a values and the orientation functions f_c and f_a deduced from X-ray and birefringence measurements, the axial (E_0) and transverse (E_{90}) Young's modulus are calculated and compared with the experimental data in Figure 13. It is seen that at -60°C (just below the γ relaxation) where the amorphous phase is rigid, the substantial increase in E_0 and the slight decrease in E_{90} with rising draw ratio is well predicted by the model. However, the quantitative agreement is not good above $\lambda = 3$. At 0°C

(about midway between the γ and β relaxations) the discrepancy increases slightly but at 50°C (just above the β relaxation) the predicted values for both E_0 and E_{90} are much lower than the experimental data. Similar discrepancies, in varying degree, have been observed in our previous work on polypropylene,¹⁷ polyoxymethylene,²⁵ and nylon 6.²⁶ Although some error may arise from the uncertainty of the f_a values and the approximations used in reducing the general theoretical expression to a two-parameter form, the major part of the deviation results from the assumption of uniform stress in the calculation.

An isotropic semicrystalline polymer may be regarded a composite material in which the crystalline lamellae are dispersed in an amorphous matrix, and so the Reuss uniform stress (lower bound) model is quite adequate for understanding its mechanical behavior.^{29,42} As the polymer is moderately drawn, the chains in the crystalline and amorphous regions are gradually aligned, and there are only a small number of taut tie molecules connecting the crystallites. The stress distribution in this case can still be described roughly by the Reuss model. As the polymer is further drawn, the number of taut tie molecules increases substantially and the crystallites are more and more strongly connected. The crystalline regions then behave more like a continuous phase, and the elastic modulus deviates from the Reuss prediction and moves towards the upper bound set by the Voigt (uniform strain) model. These considerations also provide a natural explanation for the result that the discrepancy (particularly in E_{90}) becomes more serious with increasing temperature. In high temperature where the amorphous phase is rubbery, the Young's moduli predicted on the assumption of uniform stress are very low since they are largely determined by the elastic property of the soft amorphous regions. These values are not a true reflection of the mechanical properties of a highly oriented polymer since this material has an internal stress-strain field intermediate between that of uniform stress and uniform strain. Unfortunately, the above ideas cannot be further developed to provide a quantitative framework because there is very little knowledge of the stress-strain distribution in a semicrystalline polymer at any given draw ratio.

CONCLUSION

We have seen that the mechanical behavior of oriented LLDPE is mainly controlled by three factors: molecular chain orientation, stiffening effect of taut tie molecules, and *c*-shear mechanism. At low temperature where the amorphous phase is rigid, the behavior is largely determined by the overall chain orientation, which gives rise to a sharp increase in the axial Young's modulus E_0 with increasing draw ratio and slight decreases in the transverse Young's modulus E_{90} and shear modulus C_{66} . The *c*-shear process may also play a small role and leads to the drop in E_{45} and the axial shear modulus C_{44} . As the temperature rises, the amorphous phase becomes increasingly rubbery and the taut tie molecules exert a greater and greater influence until, above the β relaxation, all the elastic moduli show an increase in magnitude upon drawing. With further increase in temperature we reach the α relaxation where the *c*-shear process is the dominant mechanism. In this region, the oriented sample has very low C_{44} and E_{45} values compared to the undrawn material.

The two-phase Reuss model gives a reasonable description of the elastic behavior only at moderate draw ratio and below the major amorphous relaxation. As the draw ratio increases beyond $\lambda = 3$, the morphology changes to fibrillar and the crystalline blocks are increasingly connected by taut tie molecules. The sample thus has an internal stress-strain distribution intermediate between the uniform stress field associated with the lower bound and the uniform strain field associated with the upper bound. As the draw ratio further increases, the observed elastic moduli gradually approaches the upper bound and are therefore much higher than the Reuss values. The discrepancy between predictions and experimental results becomes more severe at high temperatures. In this region where the amorphous phase has a much lower stiffness than the crystalline phase, the elastic moduli predicted from the Reuss model are mainly related to the stiffness of the amorphous phase and thus have low values.

We wish to thank Du Pont Canada Inc. for supplying polyethylene pellets and molecular weight data.

References

1. A. Emmerich, *Plas. Technol.*, **64**, 33 (1980).
2. M. Hartung, *Plas. Technol.*, **65**, 65 (1981).
3. R. Wood, *Plast. Rubber Int.*, **6**, 15 (1981).
4. J. N. Shirrell, *Plast. Technol.*, **65**, 71 (1981).
5. C. S. Speed, *Plast. Eng.*, (Jul.), 39 (1982).
6. A. S. Manke, *Popular Plast.*, (Nov.), 11 (1983).
7. N. Fountas, *Plast. World*, (Feb.), 45 (1981).
8. R. S. Stein, T. Kyu, S. Hu, and T. Masaoka, *Polym. Prepr.*, **24**, 117 (1983).
9. D. R. Saini and A. V. Shenoy, *Polym. Commun.*, **26**, 50 (1985).
10. F. De Candia, A. Perullo, V. Vittoria, and A. Peterlin *J. Appl. Polym. Sci.*, **28**, 1815 (1983).
11. R. S. Porter, in *High Modulus Polymers and Composites*, C. L. Choy, Ed., Chinese University Press, Hong Kong, 1985.
12. C. T. Elston, DuPont of Canada, U.S. Pat. 3,645,992 (1972).
13. B. K. Hunter, K. E. Russell, M. V. Scammeli, and S. L. Thompson, *J. Polym. Sci., Polym. Chem. Ed.*, **22**, 1383 (1984).
14. B. Wunderlich and C. Cormier, *J. Polym. Sci., Polym. Phys. Ed.*, **5**, 987 (1967).
15. Z. W. Wilchinsky, in *Advances in X-Ray Analysis*, Plenum, New York, 1963, Vol. 6.
16. W. P. Leung, C. C. Chan, F. C. Chen, and C. L. Choy, *Polymer*, **21**, 1148 (1980).
17. W. P. Leung and C. L. Choy, *J. Polym. Sci., Polym. Phys. Ed.*, **21**, 725 (1983).
18. A. Peterlin, *J. Appl. Phys.*, **48**, 4099 (1977); in *Structure and Properties of Oriented Polymers*, I. M. Ward, Ed., Applied Science, London, 1975.
19. W. A. Lee and R. A. Rutherford, in *Polymer Handbook*, J. Brandrup and E. H. Immergut, Eds., Wiley-Interscience, New York, 1975.
20. C. W. Bunn and R. de P. Daubeny, *Trans. Faraday Soc.*, **50**, 1173 (1954).
21. Y. Fukui, T. Asada, and S. Onogi, *Polym. J.*, **3**, 100 (1972).
22. M. Pietralla, H. P. Grossmann, and J. K. Kruger, *J. Polym. Sci., Polym. Phys. Ed.*, **20**, 1195 (1982).
23. K. Nakayama and H. Kanetsuna, *J. Mater. Sci.*, **10**, 1105 (1975).
24. R. J. Samuels, *Structured Polymer Properties*, Wiley, New York, 1974.
25. C. L. Choy, W. P. Leung, and C. W. Huang, *Polym. Eng. Sci.*, **33**, 910 (1983).
26. W. P. Leung, K. H. Ho, and C. L. Choy, *J. Polym. Sci., Polym. Phys. Ed.*, **22**, 1173 (1984).
27. S. D. Hong, C. Chang, and R. S. Stein, *J. Polym. Sci., Polym. Phys. Ed.*, **13**, 1447 (1975).
28. W. Pechhold and H. P. Grossman, *Faraday Discuss. Chem. Soc.*, **68**, 58 (1979).
29. R. H. Boyd, *Polymer*, **26**, 323 (1985).

30. N. G. McCrum in *Molecular Basis of Transitions and Relaxations*, D. J. Meier, Ed., Gordon and Breach, New York, 1978.
31. R. Popli, M. Glotin, and L. Mandelkern, *J. Polym. Sci., Polym. Phys. Ed.*, **22**, 407 (1984).
32. H. C. Ng, W. P. Leung, and C. L. Choy, *J. Polym. Sci., Polym. Phys. Ed.*, **23**, 973 (1985).
33. Z. H. Stachurski and I. M. Ward, *J. Polym. Sci. A-2*, **6**, 1083 (1968).
34. M. Takayanagi, K. Imada, and T. Kajiyama, *J. Polym. Sci. C*, **15**, 263 (1966).
35. C. L. Choy and W. P. Leung, *J. Polym. Sci., Polym. Phys. Ed.*, **23**, 1759 (1985).
36. I. M. Ward, *Proc. Phys. Soc.*, **80**, 1176 (1962).
37. J. C. Halpin and J. L. Kardos, *J. Appl. Phys.*, **42**, 2235 (1972).
38. J. L. Kardos and J. Raison, *Polym. Eng. Sci.*, **15**, 183 (1975).
39. T. T. Wang, *J. Appl. Phys.*, **44**, 2218 (1973).
40. R. L. McCullough, C. T. Wu, J. C. Seferis, and P. H. Lindenmeyer, *Polym. Eng. Sci.*, **16**, 371 (1976).
41. J. C. Seferis and R. J. Samuels, *Polym. Eng. Sci.*, **19**, 975 (1979).
42. R. H. Boyd, *J. Polym. Sci., Polym. Phys. Ed.*, **21**, 493 (1983).
43. S. W. Tsai, J. C. Halpin, and N. J. Paganao, *Composite Materials Workshop*, Technomic, Stamford, CT, 1969.
44. I. M. Ward, *Developments in Oriented Polymers—1*, I. M. Ward, Ed. Applied Science, London, 1982.

Received February 17, 1986

Accepted February 25, 1986